Lead-free piezoelectric ceramic coatings fabricated by thermal spray process

Kui Yao, *Senior Member, IEEE*, Shuting Chen, Kun Guo, *Student Member, IEEE*, Chee Kiang Ivan Tan, Meysam Sharifzadeh Mirshekarloo, and Francis Eng Hock Tay

***Abstract*—The paper starts from a review on the progress in fabrication of piezoelectric ceramic coatings by thermal spray method. For our experimental work, two types of lead-free piezoelectric ceramic coatings, including potassium sodium niobate (KNN)-based and bismuth sodium titanate (BNT)-based, are fabricated by thermal spray process, and their structure, morphology and piezoelectric properties are characterized. Our obtained lead-free ceramic coatings exhibit single phase of perovskite structure, relatively dense morphology, and competitive piezoelectric coefficients. The mechanism of forming the piezoelectric perovskite crystalline phase by thermal spray involving melting-recrystallization process is analyzed in comparison to that of ceramic synthesis through solid state reaction. Suppression of volatile loss and decomposition at high temperature due to the extremely high melting and cooling rate in the thermal spray process, and the impact on the resulting structure are discussed. Significant advantages of the thermal spray method over alternative processing methods for forming piezoelectric ceramic coatings are summarized. The combination of environmentally friendly lead-free compositions and the scalable thermal spray processing method will promote more applications of piezoelectric ceramic coatings for producing distributive sensors and transducers, and forming advanced smart structures and systems.**

***Index Terms*—Piezoelectric materials, Thermal spray, Coatings, Ceramics, Material processing, Sensors, Transducers**

I. Introduction

THERMAL spray method is an established technique for fabricating coatings of inorganic materials in industry [1-3]. Compared to other coating methods, such as physical vapor deposition (PVD), chemical solution deposition (CSD), screen-printing and aerosol deposition (AD), thermal spray process has advantages for industry applications, such as high throughput, large area, good versatility with various types of feedstock materials, and readily forming coatings on various types of substrates [2, 3]. The current major industry application of thermal spray is for producing protective coatings, such as thermal barrier and wear-resistant coatings. Efforts of applying thermal spray method for fabrication of functional materials have been made [1], but it has never become a dominant method for producing electronic materials.

The current industrial revolution is demanding decentralized intelligence that helps create smart and interactive objects networking. However, the implementation of existing discrete sensors and transducers technologies, such as those for structural health monitoring including machine condition monitoring, is mainly based on installation of bulky, discrete and electrical wired sensors and transducers at specific locations. This is often not reliable or cost-effective in the desired cyber-physical system, and is becoming a bottleneck for advancing smart manufacturing and integrated system. Therefore, processing that can enable achieving large area smart structures and distributive sensing functions will become attractive for realizing the decentralized intelligence as demanded for the future. We are thus interested in evaluating the potential of producing piezoelectric ceramic coatings with thermal spray process.

Over the past several decades, the efforts in fabrication of piezoelectric ceramic coatings by thermal spray have not led to a thermal sprayed piezoelectric coating suitable for practical large area sensors and transducers applications, due to the limited performance properties and/or toxic compositions, as reviewed below.

Most of the reports on thermal spray-derived piezoelectric coatings are lead zirconate titanate (PZT)-based ceramics [4-11], which are the mainstay for high performance electromechanical sensors and transducers applications due to the superior piezoelectric performance from bulk PZT. Early exploration by B. Maliric *et al.* showed that coherent PZT coatings can be formed by thermal spray process, but the coatings exhibited considerable secondary phases including ZrO_2, PbO, and $PbZrO_3$, without showing any piezoelectric effect [4]. The existence of secondary phases in thermal sprayed PZT-based coatings was also reported in subsequent studies. It was understood that the formation of secondary phases is due to the incongruent melting behavior of PZT-based materials [7]. Chemical analysis by P. Ctibor *et al.* revealed that the composition of thermal sprayed PZT coating segregated to Pb-rich and Ti-rich micro-regions, which is caused by phase separation due to the incongruent melting behavior of PZT [9].

K. Yao, S. Chen, K. Guo, C. K. I. Tan and M. S. Mirshekarloo are with Institute of Materials Research and Engineering, A*STAR (Agency for Science, Technology and Research), 2 Fusionopolis Way, Innovis, Singapore 138634 (email: k-yao@imre.a-star.edu.sg).

K. Guo and F. E. H. Tay are with Department of Mechanical Engineering, National University of Singapore, 9 Engineering Drive 1, Singapore 117575.

Post spray heat treatment could enhance the perovskite phase and reduce the secondary phase, but some secondary phases, especially ZrO_2, could not be completely eliminated, leading to improved dielectric properties although piezoelectric properties were not obtained [7]. PZT coating without secondary phase was only obtained by adding 100 % excess PbO under optimized plasma condition, but still no piezoelectric effect was found in the coatings [4]. The piezoelectricity of PZT coatings was first reported by S. Sherrit *et al.*, with extremely small d_{33} of 0.47 to 1.1 pC/N only [5]. The very low piezoelectric response was attributed to the large porosity of the coatings [5]. Recently, PZT-based coatings with single phase, lower porosity and reduced physical defects were fabricated by more sophisticated supersonic plasma spray, in which the feedstock is accelerated to significantly higher speed than conventional thermal spray [11]. A piezoelectric coefficient d_{33} of 61 pC/N was reported in the PZT coatings from the supersonic plasma spray.

Besides the unsatisfactory performance properties so far, another serious concern about thermal sprayed Pb-based piezoelectric ceramic coating is the significant amount of toxic and highly volatile lead composition. The volatility of lead in the melting state during the thermal spray process is much higher than solid state ceramic sintering, which brings even more significant health and environmental issues than bulk ceramic processing.

There are efforts in fabricating ferroelectric barium titanate (BT)-based ceramic coatings by thermal spray since 2000's [12-18]. The effects of thermal spray conditions and post-spray heat treatment on the crystal structure and electrical properties of the BT-based coatings were studied in detail. However, most of the studies focused on dielectric properties of the BT coatings, and only a recent study reported piezoelectric properties of BT-based coatings with $d_{33} < 15$ pC/N [18], which were fabricated by sophisticated supersonic plasma spray. The small piezoelectric coefficient and low Curie temperature of BT limit the coatings' piezoelectric applications.

Over the last decade, extensive efforts have been made in research and development of high performance bulk ceramic of lead-free piezoelectric materials, with significant progress made in performance improvement [19-25]. A series of lead-free material systems have been reported with piezoelectric performance comparable to those of PZT-based materials. Several excellent and comprehensive reviews on lead-free piezoelectric materials are given by J. Wu *et al.*[26, 27], J. Rodel *et al.* [28] and T. R. Shrout *et al.* [29]. Among the lead-free candidates, two main types of materials, including potassium-sodium niobate (KNN)-based and bismuth sodium titanate (BNT)-based materials, are particularly attractive because of their superior piezoelectric performance [29]. KNN-based ceramics are one of the most extensively investigated lead-free piezoelectric systems due to the large piezoelectric coefficient and high Curie temperature (T_C) [19, 20, 30]. Strong piezoelectric effects competitive to the market dominant PZT have been reported in KNN-based bulk ceramics from research lab by appropriate compositional design and crystallographic phase tuning [21]. Significant progress on KNN-based piezoelectric thin films has been made through innovated chemical solution approach [31-33]. BNT-based piezoelectric ceramics are another promising lead-free materials with the advantages of high remnant polarization, large electromechanical coupling coefficient and high mechanical quality factor [29, 34, 35]. It is challenging to effectively pole pure BNT ceramic due to its high coercive field. In contrast, A-site substituted BNT-based ceramics with MPB composition possess lowered coercive field and exhibit superior electromechanical properties [28]. Among the BNT-based ceramic systems, $Bi_{0.5}(Na_{0.70}K_{0.20}Li_{0.10})_{0.5}TiO_3$ (BNKLT) composition shows superior piezoelectric properties [36]. However, to our best knowledge, there is no thermal sprayed high performance lead-free piezoelectric coating reported in the literature before we started work in this area. [37]

In our experimental work here, both BNT and KNN-based piezoelectric ceramic coatings were fabricated by thermal spray process, and their structure, morphology, and electrical properties were investigated. The mechanism of forming the perovskite phase from the melt in the thermal spray process was analyzed in comparison with solid state synthesis reaction in ceramic process. Different coating fabrication methods for producing piezoelectric ceramic coatings were compared, and the results and analyses showed thermal spray process is a promising method for producing lead-free piezoelectric coatings for industry applications.

II. Process of Coating by Thermal Spray

As schematically illustrated in Fig. 1, during thermal spray, materials in the form of powder, rod or wire are injected to a heat source (e.g. plasma) in which they are heated to near or above their melting temperature. The resulting molten or semi-molten material is accelerated by a gas stream and the spray stream is projected against the substrate surface to be coated. Particles with high thermal and kinetic energy impact and solidify on the surface, with coating build-up by overlapping and interlocking during solidification, as illustrated in the inset of Fig. 1. Coatings with a large range of thickness can be achieved in multiple passes of the torch over the substrate. Thermal sprayed coatings are often subjected to post-spray processing to achieve desired structure and properties. The processing includes thermal treatment (e.g. heat treatment, hot isostatic pressing), mechanical treatment (e.g. short peening), and chemical treatment (e.g. organic sealing). Thermal spray is compatible with various types of substrate without thermal distortion effect, and is able to deposit coatings on a substrate without significant heating effect. Virtually any material that melts without decomposition can be used.

Among the various types of thermal spray process, Atmospheric Plasma Spraying (APS) is mainly used for fabrication of piezoelectric ceramic coatings [4, 5, 13, 17]. In APS process, a gas, such as argon, is introduced to a cathode and an anode, wherein an electric arc is initiated between the electrodes. The arc ionized the gas, creating high pressure plasma with a temperature of a few thousand degree or even higher. Feedstock is introduced to the plasma, heated, and

accelerated by the high temperature and high velocity plasma stream. Recently, fabrication of piezoelectric ceramic coating using a customized supersonic plasma spray system has been explored. The specially designed spraying gun enables particle velocity significantly higher than that of APS, resulting in coatings with significantly reduced porosity.

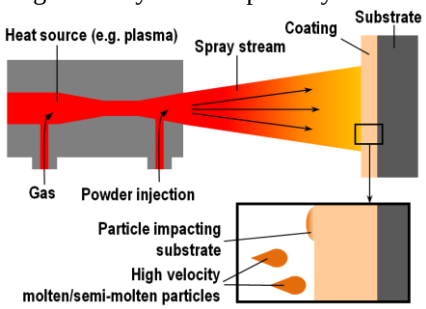

Fig. 1. Schematic illustration of thermal spray process

A.H. Dent *et al.* explored High Velocity Oxy-Fuel (HVOF) for fabrication of BT-based coatings [12]. In HVOF process, fuel, such as propane and liquid kerosene, is mixed with oxygen and burned in a chamber, and the resulting combustion flame is introduced to a nozzle where the gas velocities may reach supersonic. Feedstock is heated and accelerated in the nozzle and projected towards the substrate. Coatings with smoother surface and better density can be achieved by this method because of the high kinetic energy of the particles. Since the flame temperature is substantially lower than that of plasma spray, HVOF is not suitable for spraying materials with high melting point.

III. Results of Lead-Free Piezoelectric Ceramic Coatings by Thermal Spray

KNN-based feedstock with composition of $(K_{0.44}Na_{0.52}Li_{0.04})(Nb_{0.84}Ta_{0.10}Sb_{0.06})O_3$ (KNN-LiTaSb) was prepared with starting material of K_2CO_3 (99.5 %), Na_2CO_3 (99.0 %), Li_2CO_3 (99.999 %), Nb_2O_5 (99.9 %), Ta_2O_5 (99.85 %), Sb_2O_5 (99.998 %). 10 mol% excess potassium and sodium were introduced into the starting materials to compensate the volatile loss. Details of the preparation of the feedstock can be found in our recent publication [37]. BNT-based feedstock with composition of $Bi_{0.5}(Na_{0.70}K_{0.20}Li_{0.10})_{0.5}TiO_3$ (BNKLT) was prepared with starting materials of Bi_2O_3 (99.99 %), Na_2CO_3 (99.5 %), TiO_2 (99.90 %), Li_2CO_3 (99.998 %) and K_2CO_3 (99 %). Excess 10 mol% bismuth was introduced into the starting materials to compensate the volatile loss. The starting materials were mixed in ethanol according to the stoichiometry and milled for 24 h by a planetary ball-mill machine. After drying, the mixture was calcined in a furnace at 850 °C for 2 h.

The feedstock was fed into the torch of an Atmospheric Plasma Spray system (9MC, Sulzer Metco Inc. US) and deposited onto alumina substrates with screen-printed Ag/Pd (70/30) electrodes. The coatings were deposited at plasma power of 23 kW and 17 kW, for KNN-LiTaSb and BNKLT feedstock, respectively, with torch-substrate distance of 120 mm and feeding rate of 20 g/min. Thicknesses of the KNN-LiTaSb and BNKLT coatings were 90 µm and 75 µm, respectively. In order to enhance crystallinity of perovskite structure, some of the KNN-LiTaSb and BNKLT coatings were heat-treated at 1150 °C and 1100 °C for 30 min, respectively.

Crystal structure of the feedstock and thermal sprayed coatings were analyzed by X-ray diffraction (XRD, Bruker D8 General Area Detector Diffraction System, Germany). As presented in Fig. 2, both KNN-LiTaSb and BNKLT feedstocks showed single phase of perovskite structure. The as-sprayed KNN-LiTaSb and BNKLT coatings also exhibited single phase of perovskite structure, with minor diffraction humps attributed to amorphous phase in the coatings. After heat treatment, both KNN-LiTaSb and BNKLT coatings showed single phase of perovskite structure with significantly increased intensity of diffraction peaks compared with the as-sprayed coatings, indicating the enhanced crystallinity by the heat treatment.

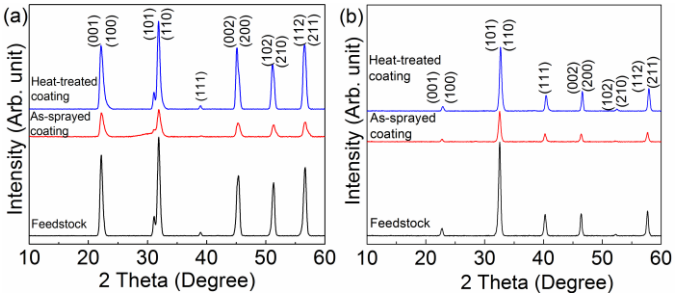

Fig. 2. XRD patterns of (a) KNN-LiTaSb feedstock and thermal sprayed coatings, and (b) BNKLT feedstock and thermal sprayed coatings.

The surface and cross-sectional morphology of the coatings were examined by Field Emission Scanning Electron Microscopy (FESEM, JEOL 7600, Japan). As presented in Fig. 3(a), the as-sprayed KNN-LiTaSb coating showed dense morphology with smooth surface. The smooth features were mainly formed by the rapid solidification of the molten powder during coating build up, with substantial amorphous phase due to the rapid quenching from molten state. Cross-sectional inspection revealed smooth features with considerable cubic-shaped crystals in the coatings, as shown in Figs. 3(b) and 3(c), indicating the formation of KNN-LiTaSb piezoelectric crystals directly by thermal spray. The coating after heat treatment exhibited different morphology. As revealed in Figs. 3(d), 3(e) and 3(f), the dominant structure of the heat-treated coating is cubic-shaped grains with size significantly larger than that of the as-sprayed coatings, indicating enhanced crystallinity of the perovskite structure due to the heat treatment, which is consistent with the XRD results.

FESEM images of the BNKLT coatings are presented in Fig. 4. Mixture of large spherical features and small cubic-shaped grains were observed on the surface of the as-sprayed BNKLT coatings, as shown in Fig. 4(a). The spherical features are believed to be formed by the rapid solidification of the molten powder during coating build up, which is similar to the smooth features observed in the as-sprayed KNN-LiTaSb coatings shown in Figs. 3(a) and 3(c). The BNKLT coatings after heat treatment exhibited cubic-shaped grains with size significantly larger than that of as-sprayed coatings, as shown in Figs. 4(b)

and 4(c), indicating enhanced crystallinity of the perovskite structure due to the heat treatment. It is noted that the BNKLT coatings exhibited denser morphology than the KNN-LiTaSb coatings.

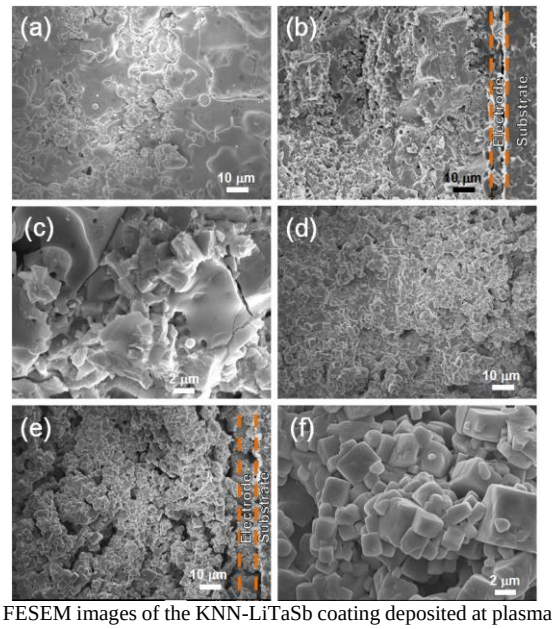

Fig. 3. FESEM images of the KNN-LiTaSb coating deposited at plasma power of 23 kW: (a) surface of the as-sprayed coating, (b) and (c) cross-section of the as-sprayed coating, (d) surface of the heat-treated coating, (e) and (f) cross-section of the heat-treated coating.

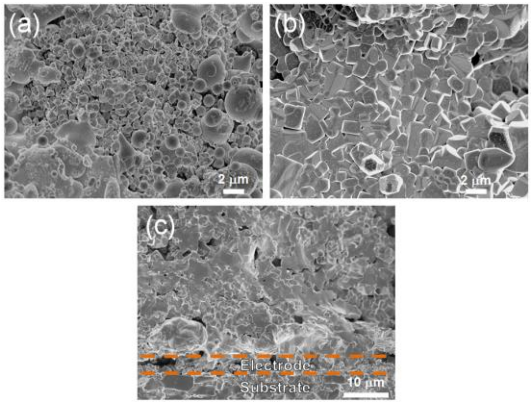

Fig. 4. FESEM images of the thermal sprayed BNKLT coating: (a) surface of the as-sprayed coating, (b) surface and (c) cross-section of the heat-treated coating.

The as-sprayed coatings typically showed low dielectric constant, high dielectric loss, and small ferroelectric polarization due to the low crystallinity. After the heat treatment, the electrical properties were significantly improved. The KNN-LiTaSb and BNKLT coatings exhibited dielectric constant / loss of 720 / 0.06 and 1050 / 0.05, respectively, at 10 kHz and room temperature.

The KNN-LiTaSb and BNKLT coatings were poled at 100 °C by a DC electric field of 15 kV/cm for 8 min and 40 kV/cm for 10 min, respectively. The piezoelectric properties of the coatings were characterized by a laser scanning vibrometer (OFV-3001-SF6, PolyTech GmbH, Germany), which is an established method for determining d_{33} of piezoelectric films with a substrate [38]. Weak piezoelectric response was observed in the as-sprayed coatings, with an effective piezoelectric coefficient (d_{33}) of 4~5 pC/N measured in both KNN-LiTaSb and BNKLT coatings under substrate clamping condition. Significantly stronger piezoelectric response was obtained after heat-treat for both coatings. Fig. 5 presents three-dimensional drawings of the instantaneous vibration data when the displacement magnitude of the heat-treated KNN-LiTaSb and BNKLT coatings reached the maximum under electric sine wave driving at 1 kHz with voltage amplitudes of 10 V and 20 V, respectively. The corresponding effective piezoelectric coefficients (d_{33}) of the KNN-LiTaSb and BNKLT coatings were 112 pC/N, and 75 pC/N, respectively under substrate clamping effect.

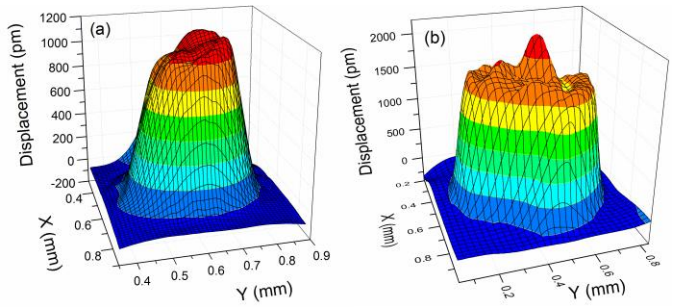

Fig. 5. Three-dimensional drawings of the instantaneous vibration data when the displacement magnitude of the thermal sprayed coating reaches the maximum under electric driving: (a) KNN-LiTaSb coating, and (b) BNKLT coating.

IV. Discussion

The mechanism of forming piezoelectric ceramic coatings by thermal spray method involving the melting process is distinct from that of ceramic synthesis by conventional solid state reaction. The major differences of these two methods are schematically illustrated in Fig. 6 with KNN-based material as an example. Synthesizing KNN-based ceramics by solid state reaction involves decomposition of carbonates followed by diffusion-controlled solid state reaction [25]. The carbonates in the starting materials are first decomposed to reactive alkaline oxides:

$$A_2CO_3 \rightarrow A_2O + CO_2$$

where A represents K, Na. The reaction is followed by diffusion of alkaline and oxygen ions from the alkaline oxides to B_2O_5, where B represents Nb, to form intermediate product of $A_2B_4O_{11}$:

$$A_2O + 2B_2O_5 \rightarrow A_2B_4O_{11}$$

Further reaction involves diffusion of alkaline and oxygen ions into B_2O_5 to form perovskite crystals (ABO_3):

$$A_2O + A_2B_4O_{11} \rightarrow 4ABO_3$$

Both the decomposition of carbonates and reaction of forming perovskite crystals are diffusion-controlled, involving

ion diffusion over a long distance through the multiple intermediate and product phases, as shown in Fig. 6(a). As a result, the reactions of forming perovskite crystals by solid state reaction are intrinsically slow, particularly in the cases of inhomogeneous mixing of reactants or use of reactants with large particle size.

In contrast, the formation of piezoelectric ceramic coatings by thermal spray of the perovskite feedstock only requires short range diffusion of ions, as shown in Fig. 6(b). In the process of fabricating KNN-based coatings by thermal spray, the feedstock, which is already in perovskite structure, is heated to molten or semi-molten state and subsequently solidified on the substrate and re-crystallized into perovskite structure. This process can be described by the reaction formula below:

$$ABO_3\,(\text{solid}) \rightarrow ABO_3\,(\text{liquid}) \rightarrow ABO_3\,(\text{solid})$$

where A represents K, Na, and B represents Nb. During thermal spray, the melting of feedstock and the subsequent solidification occur in very short period. Therefore, the ionic coordination of the melt may still maintain the short range order similar to that of the original perovskite structure, as indicated by the formula of ABO_3 (liquid). The literature of structural analyses on $KNbO_3$ and $LiNbO_3$ in molten state reported that local ordering clusters of NbO_6 (basic unit of perovskite structure) exist in the melt as well as at crystal-melt interface [39, 40]. Because of the short range order existing in the melt, crystallization of perovskite structure in thermal spray process is kinetically more favorable in addition to the thermodynamic preference, as it mainly involves slight local shift of ions without the long distance diffusion through the multiple intermediate and product phases.

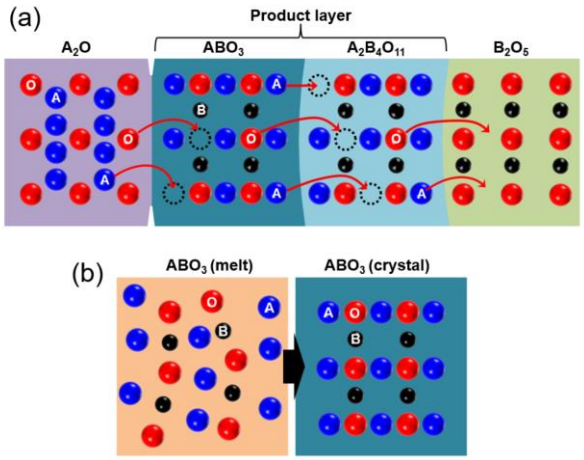

Fig. 6. Schematic illustration of forming KNN-based ceramics: (a) by conventional solid state reaction, and (b) by thermal spray involving melting and recrystallization. A represents K, Na, and B represents Nb.

To study the melt-solidification and recrystallization behavior of the feedstock during thermal spray, the BNKLT feedstock was characterized by simultaneous Differential Scanning Calorimetry (DSC) and Thermogravimetry (TG) analysis (STA 449 F1 Jupiter, Netzsch GmbH, Germany). The feedstock was heated to 1400 °C with a heating rate of 20 °C /min, followed by cooling at the same rate. As presented in Fig. 7(a), during the heating process, there is a broad endothermic peak between 1100 °C to 1260 °C associated with melting of the feedstock, and a significant weight loss was observed accompanied by melting as observed in the TG curve.

The significant weight loss was continued when the feedstock remained melt during the subsequent cooling process until temperature dropped to ~1186 °C corresponding to recrystallization of BNKLT perovskite phase, as presented in Fig. 7(b). The weight loss could be mainly associated with decomposition of the powder and evaporation of volatile compositions, particularly aggravated in melting stage. The large weight loss as observed resulted in substantial deviation of the chemical composition from the desired stoichiometry, and thus formation of secondary phases during solidification. As shown in Fig. 7(b), during the cooling process, multiple small exothermic peaks were observed below the main perovskite phase crystallization peak at 1186 °C, which are attributed to crystallization of the secondary phases. XRD analysis on the feedstock going through the same heating-melting-cooling process as in the DSC-TG analysis revealed at least three secondary phases, including Li_2TiO_3, $NaBiTi_6O_{14}$ and Bi_2O_3, besides the main BNT perovskite phase, as presented in Fig. 8.

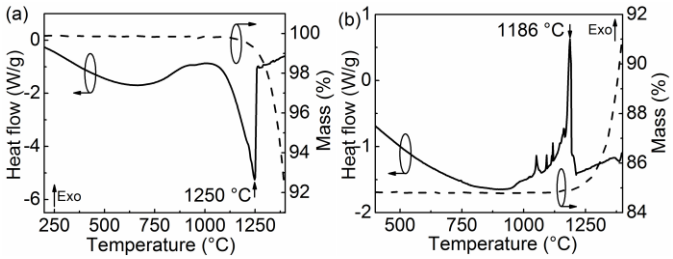

Fig. 7. DSC-TG curves of BNKLT feedstock in (a) heating and (b) cooling process.

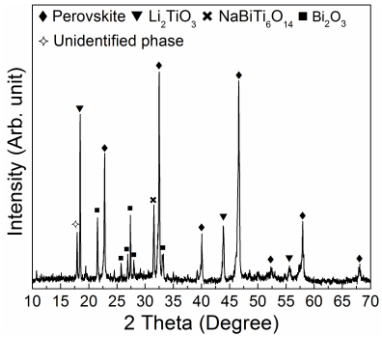

Fig. 8. XRD pattern of the BNKLT feedstock after the same heating-melting-cooling cycle as in the thermal analysis.

Despite the fact that a substantial amount of multiple secondary phases was present in the feedstock going through the same heating-melting-cooling process as in the DSC-TG analysis, it should be highlighted that the thermal sprayed BNKLT coating derived from the same feedstock material did not show secondary phases apparently (refer to Fig. 2(b)). This should be mainly due to the significant difference in the heating and cooling rate involved in the two processes. The heating-melting-cooling process as in the DSC-TG analysis is ~20

°C/min and the total time in the melting state with the aggravated volatile loss is ~10^3 sec. In contrast, the duration of melting during thermal spray is very short, less than few milliseconds (~10^{-3} sec) [41]. Thus, the loss of volatile composition and decomposition of the BNKLT thermal sprayed coatings could be significantly suppressed, resulting in recrystallization occurrence at the composition close to the desired chemical stoichiometry with minimized secondary phase.

Based on experimental results and analyses, a comparison of the characteristics of different processing methods for fabricating lead-free piezoelectric ceramic coatings is given in Table I, together with effective piezoelectric coefficient d_{33} of the resulting coatings. Physical vapor deposition (PVD), such as sputtering and pulsed laser deposition (PLD) [42, 43], is an extensively studied process to grow thin films with small thickness, typically < 2 μm, due to its low deposition rate. It is challenging to deposit films on large substrates or those with complex structure by PVD. Chemical solution deposition (CSD) is able to fabricate thin films with complex stoichiometry and extensively studied for fabrication of piezoelectric ceramic thin films [42]. However, the typical thickness of CSD derived thin films is below 2 μm due to its low throughput and considerable residue stress exists in the film [32]. In addition, as the precursor solutions and solution coating process are usually sensitive to environmental conditions such as humidity and particles [44], CSD processing is typically conducted in controlled dry and clean atmosphere. Because both the PVD and CSD process methods require smooth substrate surface under well controlled atmosphere and can only produce uniform piezoelectric thin films over relative small area, they are mainly used for fabricating miniaturized sensors and actuators through wafer-based processing, such as for micro-electromechanical systems (MEMS) [45, 46]. Aerosol Deposition (AD) is a processing method explored for fabricating piezoelectric coatings thicker than those produced by PVD and CSD. In AD process, nanometer-sized ceramic particles are aerosolized and accelerated by high pressure carrier gas in vacuum and impinge on substrate in high speed to form ceramic coatings [47, 48]. The ceramic coatings exhibit high density, with typical thickness of 1 to 20 μm. AD-derived piezoelectric ceramic coatings with large piezoelectric coefficients have been reported [48, 49]. However, vacuum chamber condition as required in AD process limits the coating area, productivity, and the application. Screen printing is a low cost and high throughput fabrication process for fabrication of patterned piezoelectric ceramic coatings [50]. It is convenient to deposit ceramic coatings in normal open air with thickness of 10 – 50 μm, and is used for fabrication of piezoelectric thick film sensors, actuators and energy harvesters [51, 52]. However, it is not applicable for deposition on substrates with complex shape, and the need of using stencils and squeegee limits its application for large area deposition. With organic binder added in the paste, the piezoelectric thick films derived from screen-printing is typically porous, and additional complex process, such as iso-static pressure [53] and infiltration process [54], are often applied to improve the density and properties of the screen-printed thick films.

TABLE I
COMPARISON AMONG DIFFERENT PROCESSING METHODS FOR FABRICATING LEAD-FREE PIEZOELECTRIC CERAMIC COATINGS, AND PIEZOELECTRIC COEFFICIENT OF THE RESULTING COATINGS

Process	Throughput	Deposition area	Deposition environment	Substrate requirement	Typical Thickness (μm)	Piezoelectric d_{33} (pC/N)*
Physical vapor deposition	Low	Small	Vacuum	Smooth surface	< 2	58 [55], 64.5 [56]
Chemical solution deposition	Low	Small	Dry/clean air	Smooth surface	< 2	74.0 [32], 83.1 [57], 83.3 [33]
Aerosol deposition	Medium	Small	Vacuum	Complex shape	1 – 20	50 [58], 110 [49]
Screen-printing	High	Small	Normal open air	Flat substrate	10 – 50	82.5 [53]**, 110 [54]**
Thermal spray	High	Large	Normal open air	Complex shape	10 – 200	75 and 112 (this study)

*The d_{33} coefficients cited were determined by either laser interferometer or d_{33} meter, both for characterization over macro-scale area.
** Additional complex process is applied, such as iso-static pressure or infiltration process.

In contrast to the methods described above, thermal spray is a high throughput processing method for fabricating large area ceramic coatings on substrates with complex shapes and high roughness in normal open air. It can produce coatings with a large range of thickness from tens of micrometers to hundreds of micrometers. Our experimental results here demonstrated excellent piezoelectric properties from the thermal sprayed lead-free ceramic coatings. No complicated processing for scale up such as iso-static pressure [53] and infiltration process [54] is required to achieve the competitive piezoelectric coefficient data. The combination of environmentally friendly lead-free compositions and the scalable thermal spray processing method is promising to extend the applications of piezoelectric ceramic materials for producing distributive sensors and transducers, and forming advanced smart structures and systems.

V. Conclusion

KNN-LiTaSb and BNKLT lead-free piezoelectric ceramic coatings were fabricated by thermal spray process. The obtained KNN-LiTaSb and BNKLT coatings exhibited single phase of perovskite structure, dense morphology, and large

effective piezoelectric coefficients d_{33} of 112 pC/N and 75 pC/N, respectively, measured by laser scanning method under substrate clamping effect. The mechanism of forming piezoelectric ceramic materials by thermal spray involving melting-recrystallization process was analyzed in comparison to that of ceramic synthesis through solid state reaction. The recrystallization of the perovskite phase in thermal spray process only involves local shift of ions, in contrast to long distance diffusion solid state reaction in conventional ceramic synthesis. Despite the strong volatility and decomposition observed during the melting stage of the lead-free piezoelectric ceramic feedstock materials, the volatile loss and decomposition are significantly suppressed due to the extremely high melting and cooling rate in the thermal spray process, leading to the apparently single phase perovskite structures in our obtained thermal sprayed KNN-LiTaSb and BNKLT ceramic coatings.

Compared to alternative processing methods for forming piezoelectric ceramic coatings, the thermal spray method has advantages of high throughput, large coating area, and ability of producing coatings with a large range of thickness on various types of substrates under normal open air environment. The combination of environmentally friendly lead-free compositions and the scalable thermal spray processing method will inspire the applications of piezoelectric ceramic materials for producing distributive sensors and transducers, and forming advanced smart structures and systems.

VI. Acknowledgement

This project is partially supported by Singapore Maritime Institute under the Asset Integrity & Risk Management (AIM) R&D Programme, Project ID: SMI-2015-OF-01, and IMRE/15-9P1115.

VII. References

[1] S. Sampath, "Thermal spray applications in electronics and sensors: past, present, and future," *J. Therm. Spray Technol.,* vol. 19, no. 5, pp. 921-949, Sep. 2010.

[2] S. Sampath, U. Schulz, M. O. Jarligo, and S. Kuroda, "Processing science of advanced thermal-barrier systems," *MRS Bull.,* vol. 37, no. 10, pp. 903-910, Oct. 2012.

[3] H. Herman, S. Sampath, and R. McCune, "Thermal spray: Current status and future trends," *MRS Bull.,* vol. 25, no. 7, pp. 17-25, Jul. 2000.

[4] B. Malric, S. Dallaire, and K. El-Assal, "Crystal structure of plasma-sprayed PZT thick films," *Mater. Lett.,* vol. 5, no. 7-8, pp. 246-249, Jul. 1987.

[5] S. Sherrit, C. R. Savin, H. D. Wiederick, B. K. Mukherjee, and S. E. Prasad, "Plasma‐Sprayed lead zirconate titanate‐glass composites," *J. Am. Ceram. Soc.,* vol. 77, no. 7, pp. 1973-1975, Jul. 1994.

[6] W. Haessler, R. Thielsch, and N. Mattern, "Structure and electrical properties of PZT thick films produced by plasma spraying," *Mater. Lett.,* vol. 24, no. 6, pp. 387-391, Sep. 1995.

[7] R. Thielsch, W. Hassler, and W. Bruckner, "Electrical properties and mechanical stress of thick plasma-sprayed $Pb(Zr_{0.58}Ti_{0.42})O_3$ coatings," *Phys. Status Solidi A,* vol. 156, no. 1, pp. 199-207, Jul. 1996.

[8] A. K. Keshri, S. R. Bakshi, Y. Chen, T. Laha, X. Li, C. Levy, and A. Agarwal, "Nanomechanical behaviour of plasma sprayed PZT coatings," *SURF ENG,* vol. 25, no. 4, pp. 270-275, May. 2009.

[9] P. Ctibor, Z. Pala, H. Boldyryeva, J. Sedlacek, and V. Kmetik, "Microstructure and properties of plasma sprayed lead zirconate yitanate (PZT) ceramics," *Coatings,* vol. 2, no. 2, pp. 64-75, Jun. 2012.

[10] Z. G. Xing, H. D. Wang, B. S. Xu, G. Z. Ma, Y. F. Huang, J. J. Kang, and L. N. Zhu, "Structural integrity and ferroelectric-piezoelectric properties of $PbTiO_3$ coating prepared via supersonic plasma spraying," *Mater. Des.,* vol. 62, pp. 57-63, Oct. 2014.

[11] G. Li, L. Gu, H. Wang, Z. Xing, and L. Zhu, "Microstructures and dielectric properties of PZT coatings prepared by cupersonic plasma spraying," *J. Therm. Spray Technol.,* vol. 23, no. 3, pp. 525-529, Feb. 2014.

[12] A. Dent, A. Patel, J. Gutleber, E. Tormey, S. Sampath, and H. Herman, "High velocity oxy-fuel and plasma deposition of $BaTiO_3$ and $(Ba,Sr)TiO_3$," *Mater. Sci. Eng., B,* vol. 87, no. 1, pp. 23-30, Oct. 2001.

[13] K. Ahn, B. W. Wessels, and S. Sampath, "Interfacial layer effects in $Ba_{1-x}Sr_xTiO_3$ thick films prepared by plasma spray," *Mat. Res. Soc. Symp. Proc.,* vol. 758, pp. 85-90, Jan. 2002.

[14] K. Ahn, B. W. Wessels, and S. Sampath, "Dielectric properties of plasma-spray-deposited $BaTiO_3$ and $Ba_{0.68}Sr_{0.32}TiO_3$ thick films," *J. Mater. Res.,* vol. 18, no. 5, pp. 1227-1231, May. 2003.

[15] P. Ctibor, H. Ageorges, J. Sedlacek, and R. Ctvrtlik, "Structure and properties of plasma sprayed $BaTiO_3$ coatings," *Ceram. Int.,* vol. 36, no. 7, pp. 2155-2162, Sep. 2010.

[16] S. E. Hao, C. Y. Wang, D. S. Fu, J. S. Zhang, Y. A. Wei, and W. L. Wang, "Preparation and characterization of La-doped $Ba_{(1-x)}Sr_xTiO_3$ powders and thin films," *Thin Solid Films,* vol. 518, no. 20, pp. 5645-5648, Aug. 2010.

[17] P. Ctibor, H. Seiner, J. Sedlacek, Z. Pala, and P. Vanek, "Phase stabilization in plasma sprayed $BaTiO_3$," *Ceram. Int.,* vol. 39, no. 5, pp. 5039-5048, Jul. 2013.

[18] Z. Xing, H. Wang, L. Zhu, X. Zhou, and Y. Huang, "Properties of the $BaTiO_3$ coating prepared by supersonic plasma spraying," *J. Alloys Compd.,* vol. 582, pp. 246-252, Jan. 2014.

[19] X. P. Wang, J. G. Wu, D. Q. Xiao, J. G. Zhu, X. J. Cheng, T. Zheng, B. Y. Zhang, X. J. Lou, and X. J. Wang, "Giant Piezoelectricity in Potassium-Sodium Niobate Lead-Free Ceramics," *J. Am. Chem. Soc.,* vol. 136, no. 7, pp. 2905-2910, Feb. 2014.

[20] J. G. Wu, D. Q. Xiao, and J. G. Zhu, "Potassium-Sodium Niobate Lead-Free Piezoelectric Materials: Past, Present, and Future of Phase Boundaries," *Chemical Reviews,* vol. 115, no. 7, pp. 2559-2595, Apr. 2015.

[21] K. Xu, J. Li, X. Lv, J. Wu, X. Zhang, D. Xiao, and J. Zhu, "Superior piezoelectric properties in potassium–sodium niobate lead‐free ceramics," *Adv. Mater.,* vol. 28, no. 38, pp. 8519-8523, Oct. 2016.

[22] Y. Saito, H. Takao, T. Tani, T. Nonoyama, K. Takatori, T. Homma, T. Nagaya, and M. Nakamura, "Lead-free piezoceramics," *Nature,* vol. 432, no. 7013, pp. 84-87, Nov. 2004.

[23] C. K. I. Tan, K. Yao, and J. Ma, "Effects of ultrasonic irradiation on the structural and electrical properties of lead-free $0.94(K_{0.5}Na_{0.5})NbO_3$-$0.06LiNbO_3$ ceramics," *J. Am. Ceram. Soc.,* vol. 94, no. 3, pp. 776-781, Mar. 2011.

[24] C. K. I. Tan, K. Yao, P. C. Goh, and J. Ma, "$0.94(K_{0.5}Na_{0.5})NbO_3$-$0.06LiNbO_3$ piezoelectric ceramics prepared from the solid state reaction modified with polyvinylpyrrolidone (PVP) of different molecular weights," *Ceram. Int.,* vol. 38, no. 3, pp. 2513-2519, Apr. 2012.

[25] C. K. I. Tan, Y. Jiang, D. C. C. Tan, K. Yao, and T. Sritharan, "Reaction kinetics for lead-free $0.94(K_{0.5}Na_{0.5})NbO_3$-$0.06LiNbO_3$ ceramic synthesis with ultrasonic irradiation," *Int. J. Appl. Ceram. Technol.,* vol. 12, pp. E43-E48, Jan-Feb. 2015.

[26] J. G. Wu, D. Q. Xiao, and J. G. Zhu, "Potassium-sodium niobate lead-free piezoelectric ceramics: Recent advances and perspectives," *J. Mater. Sci. Mater. Electron.,* vol. 26, no. 12, pp. 9297-9308, Dec. 2015.

[27] J. G. Wu, D. Q. Xiao, and J. G. Zhu, "Potassium-sodium niobate lead-free piezoelectric materials: Past, present, and future of phase

boundaries," *Chem. Rev.*, vol. 115, no. 7, pp. 2559-2595, Apr. 2015.

[28] J. Rodel, W. Jo, K. T. P. Seifert, E. M. Anton, T. Granzow, and D. Damjanovic, "Perspective on the development of lead-free piezoceramics," *J. Am. Ceram. Soc.*, vol. 92, no. 6, pp. 1153-1177, Jun. 2009.

[29] T. R. Shrout, and S. J. Zhang, "Lead-free piezoelectric ceramics: Alternatives for PZT?," *J. Electroceram.*, vol. 19, no. 1, pp. 113-126, Oct. 2007.

[30] L. Y. Wang, W. Ren, P. Shi, and X. Q. Wu, "Structures, electrical properties, and leakage current behaviors of un-doped and Mn-doped lead-free ferroelectric $K_{0.5}Na_{0.5}NbO_3$ films," *J. Appl. Phys.*, vol. 115, no. 3, Jan. 2014.

[31] L. Wang, K. Yao, P. C. Goh, and W. Ren, "Volatilization of alkali ions and effects of molecular weight of polyvinylpyrrolidone introduced in solution-derived ferroelectric $K_{0.5}Na_{0.5}NbO_3$ films," *J. Mater. Res.*, vol. 24, no. 12, pp. 3516-3522, Dec. 2009.

[32] P. C. Goh, K. Yao, and Z. Chen, "Lead-free piezoelectric $(K_{0.5}Na_{0.5})NbO_3$ thin films derived from chemical solution modified with stabilizing agents," *Appl. Phys. Lett.*, vol. 97, no. 10, pp. 102901, Sep. 2010.

[33] Y. M. Wang, K. Yao, M. S. Mirshekarloo, and F. E. H. Tay, "Effects and mechanism of combinational chemical agents on solution-derived $K_{0.5}Na_{0.5}NbO_3$ piezoelectric thin films," *J. Am. Ceram. Soc.*, vol. 99, no. 5, pp. 1631-1636, May. 2016.

[34] X. M. Liu, and X. L. Tan, "Giant strains in non-textured $(Bi_{1/2}Na_{1/2})TiO_3$-based lead-free ceramics," *Adv. Mater.*, vol. 28, no. 3, pp. 574-+, Jan. 2016.

[35] Y. Liu, W. Ren, J. Zhao, L. Wang, P. Shi, and Z.-G. Ye, "Effect of sintering temperature on structural and electrical properties of lead-free BNT–BT piezoelectric thick films," *Ceram. Int.*, vol. 41, pp. S259-S264, Jul. 2015.

[36] D. M. Lin, D. Q. Xiao, J. G. Zhu, and P. Yu, "Piezoelectric and ferroelectric properties of $Bi_{0.5}(Na_{1-x-y}K_xLi_y)_{0.5}TiO_3$ lead-free piezoelectric ceramics," *Appl. Phys. Lett.*, vol. 88, no. 6, pp. 062901, Feb. 2006.

[37] S. T. Chen, C. K. I. Tan, and K. Yao, "Potassium-sodium niobate-based lead-free piezoelectric ceramic coatings by thermal spray process," *J. Am. Ceram. Soc.*, vol. 99, no. 10, pp. 3293-3299, Oct. 2016.

[38] K. Yao, and F. E. H. Tay, "Measurement of longitudinal piezoelectric coefficient of thin films by a laser-scanning vibrometer," *IEEE Trans Ultrason Ferroelectr Freq Control*, vol. 50, no. 2, pp. 113-116, Feb. 2003.

[39] S. M. Wan, B. Zhang, Y. L. Sun, X. L. Tang, and J. L. You, "Structural analyses of a K_2O-rich $KNbO_3$ melt and the mechanism of $KNbO_3$ crystal growth," *Crystengcomm*, vol. 17, no. 13, pp. 2636-2641, Jan. 2015.

[40] P. Andonov, P. Chieux, and S. Kimura, "A local order study of molten $LiNbO_3$ by neutron diffraction," *J. Phys. Condens. Matter.*, vol. 5, no. 28, pp. 4865-4876, Jul. 1993.

[41] J. V. Heberlein, P. Fauchais, and M. I. Boulos, *Thermal spray fundamentals: from powder to part*, New York: Springer, 2014, pp. 386.

[42] S. Trolier-McKinstry, and P. Muralt, "Thin film piezoelectrics for MEMS," *J. Electroceram.*, vol. 12, no. 1-2, pp. 7-17, Jan-Mar. 2004.

[43] K. Tsuchiya, T. Kitagawa, and E. Nakamachi, "Development of RF magnetron sputtering method to fabricate PZT thin film actuator," *PRECIS ENG*, vol. 27, no. 3, pp. 258-264, Jul. 2003.

[44] W. G. Liu, and W. G. Zhu, "Preparation and orientation control of $Pb_{1.1}(Zr_{0.3}Ti_{0.7})O_3$ thin films by a modified sol-gel process," *Mater. Lett.*, vol. 46, no. 4, pp. 239-243, Nov. 2000.

[45] G. H. Haertling, "Ferroelectric ceramics: History and technology," *J. Am. Ceram. Soc.*, vol. 82, no. 4, pp. 797-818, Apr. 1999.

[46] J. F. Scott, "Applications of modern ferroelectrics," *Science*, vol. 315, no. 5814, pp. 954-959, Feb. 2007.

[47] J. Akedo, "Room temperature impact consolidation (RTIC) of fine ceramic powder by aerosol deposition method and applications to microdevices," *J. Therm. Spray Technol.*, vol. 17, no. 2, pp. 181-198, Jun. 2008.

[48] J. J. Choi, B. D. Hahn, J. Ryu, W. H. Yoon, B. K. Lee, and D. S. Park, "Preparation and characterization of piezoelectric ceramic-polymer composite thick films by aerosol deposition for sensor application," *Sens. Actuators, A*, vol. 153, no. 1, pp. 89-95, Jun. 2009.

[49] G. Han, J. Ryu, C. W. Ahn, W. H. Yoon, J. J. Choi, B. D. Hahn, J. W. Kim, J. H. Choi, and D. S. Park, "High piezoelectric properties of KNN-based thick films with abnormal grain growth," *J. Am. Ceram. Soc.*, vol. 95, no. 5, pp. 1489-1492, May. 2012.

[50] R. Maas, M. Koch, N. R. Harris, N. M. White, and A. G. R. Evans, "Thick-film printing of PZT onto silicon," *Materials Letters*, vol. 31, no. 1-2, pp. 109-112, May. 1997.

[51] M. Ferrari, V. Ferrari, M. Guizzetti, B. Ando, S. Baglio, and C. Trigona, "Improved energy harvesting from wideband vibrations by nonlinear piezoelectric converters," *Sens. Actuators, A*, vol. 162, no. 2, pp. 425-431, Aug. 2010.

[52] Y. Jeon, J. S. Chung, and K. No, "Fabrication of PZT thick films on silicon substrates for piezoelectric actuator," *J. Electroceram.*, vol. 4, no. 1, pp. 195-199, Mar. 2000.

[53] J. Pavlic, B. Malic, and T. Rojac, "Small reduction of the piezoelectric d_{33} response in potassium sodium niobate thick films," *J. Am. Ceram. Soc.*, vol. 97, no. 5, pp. 1497-1503, May. 2014.

[54] H. Zhang, and S. Jiang, "Effect of repeated composite sol infiltrations on the dielectric and piezoelectric properties of a $Bi_{0.5}(Na_{0.82}K_{0.18})_{0.5}TiO_3$ lead free thick film," *J. Eur. Ceram. Soc.*, vol. 29, no. 4, pp. 717-723, Mar. 2009.

[55] M. D. Nguyen, M. Dekkers, E. P. Houwman, H. T. Vu, H. N. Vu, and G. Rijnders, "Lead-free $(K_{0.5}Na_{0.5})NbO_3$ thin films by pulsed laser deposition driving MEMS-based piezoelectric cantilevers," *Mater. Lett.*, vol. 164, pp. 413-416, Feb. 2016.

[56] L. S. Kang, B. Y. Kim, I. T. Seo, T. G. Seong, J. S. Kim, J. W. Sun, D. S. Paik, I. Hwang, B. H. Park, and S. Nahm, "Growth Behavior and Electrical Properties of a $(Na_{0.5}K_{0.5})$ NbO_3 Thin Film Deposited on a $Pt/Ti/SiO_2/Si$ Substrate Using RF Magnetron Sputtering," *J. Am. Ceram. Soc.*, vol. 94, no. 7, pp. 1970-1973, Jul. 2011.

[57] P. C. Goh, K. Yao, and Z. Chen, "Lithium diffusion in $(Li,K,Na)NbO_3$ piezoeletric thin films and the resulting approach for enhanced performance properties," *Appl. Phys. Lett.*, vol. 99, no. 9, pp. 092902, Aug. 2011.

[58] J. H. Ryu, J. J. Choi, B. D. Hahn, D. S. Park, and W. H. Yoon, "Ferroelectric and piezoelectric properties of $0.948(K_{0.5}Na_{0.5})NbO_3$-$0.052LiSbO_3$ lead-free piezoelectric thick film by aerosol deposition," *Appl. Phys. Lett.*, vol. 92, no. 1, Jan. 2008.